

Quantum statistical ensemble for emissive correlated systems

Alexey M. Shakirov,^{1,2} Yulia E. Shchadilova,^{1,*} and Alexey N. Rubtsov^{1,2}

¹Russian Quantum Center, Novaya 100, 143025 Skolkovo, Moscow Region, Russia

²Department of Physics, Lomonosov Moscow State University, Leninskie gory 1, 119991 Moscow, Russia

PACS numbers: 05.30.Ch, 05.70.Ln

Relaxation dynamics of complex quantum systems with strong interactions towards the steady state is a fundamental problem in statistical mechanics. The steady state of subsystems weakly interacting with their environment is described by the canonical ensemble which assumes the probability distribution for energy to be of the Boltzmann form. The emergence of this probability distribution is ensured by the detailed balance of transitions induced by interaction with the environment. Here we consider relaxation of an open correlated quantum system brought into contact with a reservoir in a vacuum state. We refer to such a system as emissive since particles irreversibly evaporate into the vacuum. The steady state of the system is a statistical mixture of stable eigenstates from which particles cannot escape due to the binding energy. We found that, despite the absence of the detailed balance, the stationary probability distribution over these eigenstates is of the Boltzmann form in each N -particle sector. A quantum statistical ensemble corresponding to the steady state is characterized by different temperatures in different sectors, in contrast to the Gibbs ensemble. We argue that the emergence of the Boltzmann distribution is rooted in a regular dependence of transition rates between eigenstates of the system on the transition energy.

Whether and how a quantum system brought out of equilibrium reaches its steady state is a fundamental question which has recently attracted much attention [1–6]. Expectation values of local observables after relaxation are typically determined by integrals of motion while the memory of microscopic details of an initial state is lost. In quantum systems the mechanism of thermalization is rooted in the properties of individual eigenstates as stated in the eigenstate thermalization hypothesis (ETH) [7–9]. The basic statement of ETH for non-integrable systems is the smoothness of eigenstate expectation values of local observables as functions of eigenenergies. For systems with integrals of motion this statement remains true if eigenstates are taken from the same subspace [10–12]. In the steady state the density matrix of any subsystem is diagonal and its elements are the same for typical initial eigenstates of the full system [13–16]. ETH may break down for rare eigenstates in the low-energy part of the spectrum [17, 18].

A subsystem weakly coupled to the rest of the system can be viewed as an open system with its surroundings acting as a reservoir. Transitions induced by coupling to the reservoir govern relaxation dynamics of the open system to the steady state which is described by the (generalized) Gibbs ensemble

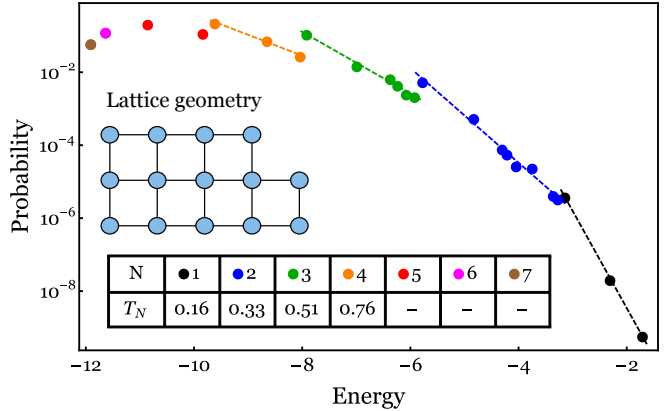


Figure 1. Stationary distribution. The plot shows a stationary probability distribution of the emissive system of hard-core bosons on a 14-site lattice (geometry is shown in the inset). The initial state of the system is the maximally occupied pure state with $N_0 = 14$. In sectors with at least 3 stable states the data is fitted with the Boltzmann distribution $P_n^N \propto \exp(-E_n/T_N)$. The temperatures T_N are presented in the table.

[19–22]. These transitions satisfy the detailed balance principle in the steady state and the probability distribution over many-body eigenstates of the open system is of the Boltzmann form. However, this general scenario does not describe a special case of an open correlated quantum system brought into contact with a reservoir in the vacuum state. In this case the detailed balance principle does not hold. We refer to such a system as emissive since particles irreversibly evaporate into the reservoir. Although particles can only leave the system, its steady state may be populated if there is a binding energy for escaping particles. If such a populated steady state is a mixture of multiple eigenstates, the probability distribution over these eigenstates is not a priori known. Thus defined quantum statistical ensemble for emissive systems has not been considered so far.

Open systems coupled to a vacuum reservoir appear ubiquitously in various fields of natural sciences including surface science [23, 24], quantum optics [25, 26], nuclear physics [27] and astrophysics [28]. In the field of cold atoms an established experimental example is a trapped atomic or molecular gas in a vacuum chamber [29–31]. Collisions of trapped particles result in internal equilibrium of the gas which alters as particles escape. The loss of particles can be accompanied by cooling. This process of evaporative cooling is a key technological development used to achieve Bose-Einstein condensation of cold atoms in magneto-optical traps [32–35]. The systems studied in experiments with ultracold atoms typically contain

* Correspondence should be addressed to yes@rqc.ru

from 10^3 to 10^6 particles. Statistical properties of these systems are usually probed by measuring their local observables. Recent experimental progress has made it possible to study smaller systems [36–39]. For these systems a direct measurement of the probability distribution over many-body states can be realized. In particular, it would allow to probe statistical properties of the steady state of emissive quantum systems.

In this paper we study an emissive quantum system of hard-core bosons on a two-dimensional lattice. We demonstrate that its probability distribution in the steady state is of the Boltzmann form in each N -particle sector. We characterize this steady state by a quantum statistical ensemble and discuss its application to calculating expectation values of observables. We show that the physical mechanism behind the emergence of the Boltzmann distribution is rooted in the behaviour of the transition rate. This rate appears to be a regular function of the transition energy though there is no detailed balance with the reservoir. We connect this behaviour with statistical properties of off-diagonal matrix elements of local annihilation operators entering expressions for transition rates.

We study a system of hard-core bosons on a two-dimensional lattice coupled to the vacuum reservoir with the Hamiltonian $H = H_S + H_R + H_I$. The lattice is described by the Hamiltonian

$$H_S = - \sum_{\langle ij \rangle} h_{ij} (b_i^\dagger b_j + b_j^\dagger b_i) \quad (1)$$

with a constraint that each site can be occupied with no more than one particle. Here b_i^\dagger (b_i) is a creation (annihilation) operator on the site i , h_{ij} are hopping amplitudes and the sum runs over the pairs of nearest-neighbour sites. For calculations we use a lattice of 14 sites (see inset of Fig. 1). To ensure non-integrability of the lattice, different values are assigned to hopping amplitudes h_{ij} . These values are taken from the interval between 0.8 and 1.2 (in arbitrary units of energy). The vacuum reservoir is described by the Hamiltonian $H_R = \sum_k \varepsilon_k a_k^\dagger a_k$ with operators a_k^\dagger (a_k) creating (annihilating) particles in reservoir modes k with energy ε_k . The interaction between the lattice and the reservoir is introduced through the Hamiltonian $H_I = \alpha \sum_{ki} (a_k^\dagger b_i + b_i^\dagger a_k) \theta(\varepsilon_k - \varepsilon_0)$, where the unit step function $\theta(\varepsilon_k - \varepsilon_0)$ accounts for the binding energy ε_0 . This binding energy is a tunable parameter in our calculations. We consider the weak coupling limit $\alpha \ll 1$ and assume that escaping particles immediately lose the coherence with the lattice and do not return back to it.

We describe the reduced dynamics of the lattice by a master equation [40, 41] for its density matrix ρ_S . The density matrix is represented in a basis of eigenstates of H_S . These eigenstates $|N, n\rangle$ are divided into sectors according to the number of particles N in the lattice. Corresponding eigenenergies are denoted by E_n^N . We consider transitions between the eigenstates generated by the coupling to the reservoir in the leading perturbative order [42]. In the absence of special symmetries of the lattice there are two constraints on these transitions: (i) $\Delta N = -1$ which is due to the type of coupling, (ii) $\Delta E < -\varepsilon_0$ which is due to the binding energy for escaping particles.

We consider the dynamics of the system at the coarse-grained time scale $dt \sim \tau_{loss}$ where τ_{loss} is the characteristic time of the particle loss process. In the weak coupling regime $\tau_{loss} \propto \alpha^{-2}$ is much larger than the dephasing time, so that only diagonal elements of the density matrix contribute to dynamics. These elements $\langle N, n | \rho_S | N, n \rangle \equiv P_n^N$ may be viewed as the probability distribution of the lattice over its eigenstates. The master equation is reduced to the system of rate equations for this probability distribution

$$\frac{d}{dt} P_n^N = \sum_m R_{nm}^{N+1} P_m^{N+1} - \sum_m R_{mn}^N P_n^N, \quad (2)$$

where R_{mn}^N is a transition rate from the state $|N, n\rangle$ into the state $|N-1, m\rangle$. For transitions allowed by selection rules the rates are estimated using Fermi's golden rule as

$$R_{mn}^N = 2\pi\Omega_0\alpha^2 \sum_{i=1}^L |\langle N-1, m | b_i | N, n \rangle|^2. \quad (3)$$

Here the step-like density of states of the reservoir $\Omega = \Omega_0\theta(\varepsilon - \varepsilon_0)$ has been used. The particle loss process can be viewed as a sequence of transitions which brings the system from the initial to one of the stable states from which no further transitions can occur (see Supplementary). There is a trivial stable state with no particles and occupied stable states which appear due to the constraint on the transition energy. For calculations we use the maximally occupied pure state with $N_0 = 14$ as the initial one and choose $\varepsilon_0 = 0$ to maximize the number of stable states (see Supplementary) which can be achieved. For the 14-site lattice this number is 26 and the maximal occupation of stable states is 7.

The probability distribution of the system in a steady state is shown in Fig. 1. In each N -particle sector of the Hilbert space (having at least 3 stable states) this stationary distribution is found to be of the Boltzmann form. We describe the steady state by a quantum statistical ensemble of the following form

$$P_n^N = \frac{P_N}{Z_N} e^{-E_n^N/T_N} \quad (4)$$

characterized by a set of temperatures T_N . Here $Z_N = \sum_n e^{-E_n^N/T_N}$ is the partial partition function which is a sum over N -particle states, P_N is the total probability in the N -particle sector. Stationary expectation values of observables are given by a standard expression $\langle A \rangle = \sum_{Nn} P_n^N \langle N, n | A | N, n \rangle$. We note that the steady state can be characterized by this statistical ensemble for an arbitrary initial state of the system (see Supplementary). Variation of the initial state only changes parameters P_N and T_N of the distribution.

The emergence of the Boltzmann distribution in the emissive system can be understood from statistics of transitions which the system undergoes as particles evaporate. For each sector we calculate occurrence probabilities of intermediate states, i.e. states through which the system evolves from the initial to one of the stable states. These distributions in sectors (referred to as intermediate) are shown in Fig. 2 as functions of the energy of the states. In sectors $N = 3 \div 11$ the dependence is smooth and fluctuations of the data are less than the

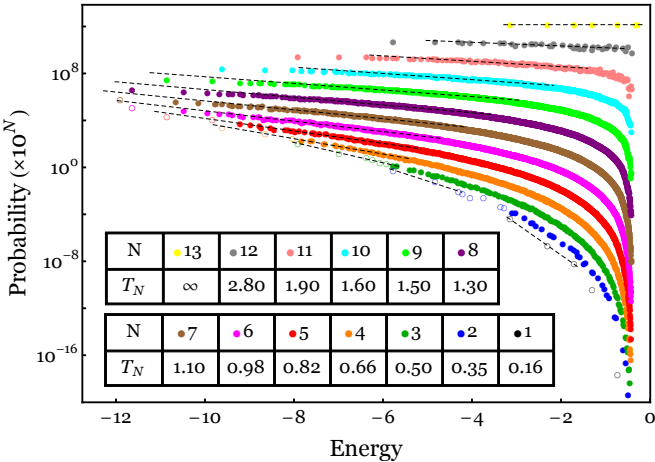


Figure 2. Intermediate distributions. The plot shows the probability distribution of intermediate states in each N -particle sector (the measurement procedure is described in the text). The initial state of the system is the maximally occupied pure state with $N_0 = 14$. For illustrative purposes the rates are multiplied by the factor 10^N . Stable states are indicated with empty circles. In each sector points accumulating 80% of the total probability are fitted with exponential functions $P_N(E) \propto \exp(-E/T_N)$. The temperatures T_N are presented in the table.

size of points. In each sector we consider the part of the spectrum accumulating the probability of $0.8P_N$ and approximate corresponding points by the Boltzmann distribution (4). For $N \leq 7$ the data includes stable states and the temperatures are close to those in Fig. 1. We note that measuring occurrence probabilities of the intermediate states will require collecting statistics from an ensemble of emissive systems. Assuming that the spectrum of the system is discrete and not degenerate, a sequence of intermediate states can be directly determined by measuring energies of escaping particles.

The smooth dependence of intermediate probability distributions on energy can be understood from the statistical properties of transition rates in the system. Fig. 3 shows R_{mn}^N plotted as a function of transition energy $\varepsilon = E_n - E_m$. In each sector data for $R^N(\varepsilon)$ can be approximated by a regular dependence with state-to-state fluctuations. For an arbitrary initial N -particle ensemble the probability distribution in $(N-1)$ -particle sector after the loss of a particle is determined by

$$P_m^{N-1} \propto \sum_n R_{mn}^N P_n^N. \quad (5)$$

Possible state-to-state fluctuations of P_n^N are convolved with the regular function of the transition energy and almost do not translate into the probability distribution in the following sector. If transition rates in neighbouring sectors are uncorrelated, the probability distribution after the loss of several particles becomes a smooth function of energy.

The analysis of lattices of different sizes (see Supplementary) shows that the transition rate is always a regular function of the transition energy with state-to-state fluctuations. The fluctuations decrease with the increase of the size of the lat-

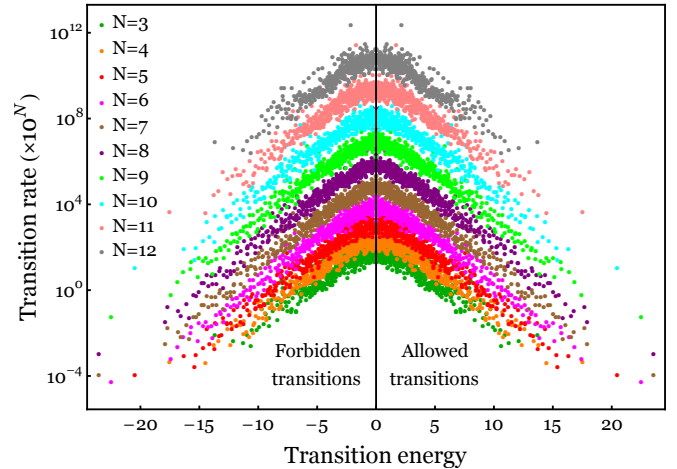


Figure 3. Transition rates. The plot shows transition rates R_{mn}^N from states in N -particle sector to states in $(N-1)$ -particle sector as a function of the transition energy $\varepsilon = E_n - E_m$ for $N = 3, \dots, 12$. Allowed transitions correspond to $\varepsilon > \varepsilon_0 = 0$. For illustrative purposes 900 points are shown for each N and the rates are multiplied by the factor 10^N .

ice. We expect that they vanish in the macroscopic limit, though it is not evident from the available range of lattice sizes. This assumption is supported by the correspondence of the system to a classical gas in a trap in the macroscopic limit. In a classical gas the probability distribution for the energy of particles is the regular exponential function. In our case the probability distribution for the energy of an escaping particle is determined by $R_{mn}^N(\varepsilon)$. Fig. 3 shows an approximately exponential dependence of R_{mn}^N on the transition energy for allowed transitions with $\varepsilon > 0$. Vanishing of fluctuations in the macroscopic limit follows from the correspondence principle.

The regular dependence of the transition rate on the transition energy relates to statistical properties of off-diagonal matrix elements $\langle N-1, m | b_i | N, n \rangle$ which enter the expression (3). It is important to note that b_i are non-Hermitian annihilation operators and matrix elements are calculated between states in different sectors, in contrast to known studies [43, 44]. We argue that the smooth dependence of these matrix elements on the transition energy is similar to the smooth dependence of eigenstate expectation values on the energy in ETH. Fluctuations of expectation values vanish as the size of the system increases [45–47]. From our scaling analysis we expect that fluctuations of $\langle N-1, m | b_i | N, n \rangle$ have the same property.

We note that the experimental verification of our findings will require measuring the probability distribution of a system under study over its many-body states. This type of measurements is in contrast to determining temperature from average values of (local) observables. While the latter is available both for finite-size and macroscopic systems, the former is only realizable for systems of finite size.

To summarize, we demonstrated an emergence of the Boltzmann distribution in each N -particle sector of an emissive system of hard-core bosons on a lattice. The steady state of the system was described by a quantum statistical ensemble char-

acterized by a set of temperatures. Smooth probability distributions are the consequence of statistical properties of transition rates in the system. Transition rates are expressed in terms of off-diagonal matrix elements of local annihilation operators and depend smoothly on the transition energy. This allowed us to draw the analogy with ETH which asserts the smooth dependence of eigenstate expectation values on the energy. We expect that this feature of transition rates is a generic property of correlated emissive quantum systems and the formation of a smooth Boltzmann distribution can be observed in contem-

porary experiments with ultracold atoms.

ACKNOWLEDGEMENTS

We are greatful to A. E. Antipov, P. V. Elyutin, P. Grišins, P. Ribeiro for useful discussions. The authors acknowledge a financial support from the RFBR grant 14-02-01219 and the Dynasty foundation.

-
- [1] S. Hofferberth, I. Lesanovsky, B. Fischer, T. Schumm, and J. Schmiedmayer, *Nature* **449**, 324 (2007).
- [2] A. Polkovnikov, K. Sengupta, A. Silva, and M. Vengalattore, *Rev. Mod. Phys.* **83**, 863 (2011).
- [3] S. Trotzky, Y.-A. Chen, A. Flesch, I. P. McCulloch, U. Schollwöck, J. Eisert, and I. Bloch, *Nat. Phys.* **8**, 325 (2012).
- [4] M. Gring, M. Kuhnert, T. Langen, T. Kitagawa, B. Rauer, M. Schreitl, I. Mazets, D. A. Smith, E. Demler, and J. Schmiedmayer, *Science* **337**, 1318 (2012).
- [5] T. Langen, R. Geiger, M. Kuhnert, B. Rauer, and J. Schmiedmayer, *Nat. Phys.* **9**, 640 (2013).
- [6] J. Eisert, M. Friesdorf, and C. Gogolin, *Nat. Phys.* **11**, 124 (2015).
- [7] J. M. Deutsch, *Phys. Rev. A* **43**, 2046 (1991).
- [8] M. Srednicki, *Phys. Rev. E* **50**, 888 (1994).
- [9] M. Rigol, V. Dunjko, and M. Olshanii, *Nature* **452**, 854 (2008).
- [10] M. Rigol, V. Dunjko, V. Yurovsky, and M. Olshanii, *Phys. Rev. Lett.* **98**, 50405 (2007).
- [11] A. C. Cassidy, C. W. Clark, and M. Rigol, *Phys. Rev. Lett.* **106**, 140405 (2011).
- [12] P. Calabrese, F. H. L. Essler, and M. Fagotti, *Phys. Rev. Lett.* **106**, 227203 (2011).
- [13] S. Popescu, A. J. Short, and A. Winter, *Nat. Phys.* **2**, 754 (2006).
- [14] N. Linden, S. Popescu, A. Short, and A. Winter, *Phys. Rev. E* **79**, 061103 (2009).
- [15] S. Genway, A. F. Ho, and D. K. K. Lee, *Phys. Rev. Lett.* **105**, 260402 (2010).
- [16] S. Genway, A. F. Ho, and D. K. K. Lee, *Phys. Rev. A* **86**, 023609 (2012).
- [17] G. Biroli, C. Kollath, and A. M. Läuchli, *Phys. Rev. Lett.* **105**, 250401 (2010).
- [18] G. Roux, *Phys. Rev. A* **81**, 53604 (2010).
- [19] S. Goldstein, J. L. Lebowitz, R. Tumulka, and N. Zanghì, *Phys. Rev. Lett.* **96**, 2 (2006).
- [20] M. Eckstein and M. Kollar, *Phys. Rev. Lett.* **100**, 120404 (2008).
- [21] M. Žnidarič, T. Prosen, G. Benenti, G. Casati, and D. Rossini, *Phys. Rev. E* **81**, 051135 (2010).
- [22] A. Riera, C. Gogolin, and J. Eisert, *Phys. Rev. Lett.* **108**, 1 (2012).
- [23] R. G. Cooks, Z. Ouyang, Z. Takats, and J. M. Wiseman, *Science* **311**, 1566 (2006).
- [24] G. A. Somorjai and Y. Li, *Introduction to surface chemistry and catalysis*. (John Wiley & Sons, 2010).
- [25] M. O. Scully and M. S. Zubairy, *Quantum optics*. (Cambridge University Press, 1997).
- [26] D. F. Walls and G. J. Milburn, *Quantum optics*. (Springer Science & Business Media, 2007).
- [27] R. P. Talevarkhan, C. D. West, J. S. Cho, R. T. Lahey, R. I. Nigmatulin, and R. C. Block, *Science* **295**, 1868 (2002).
- [28] L. Spitzer, *Dynamical evolution of globular clusters*. (Princeton University Press, 1987).
- [29] M.-O. Mewes, M. R. Andrews, D. M. Kurn, D. S. Durfee, C. G. Townsend, and W. Ketterle, *Phys. Rev. Lett.* **78**, 582 (1997).
- [30] I. Bloch, *Nat. Phys.* **1**, 23 (2005).
- [31] I. Bloch, T. W. Haensch, and T. Esslinger, *Phys. Rev. Lett.* **82** (1999), 10.1103/PhysRevLett.82.3008.
- [32] H. F. Hess, *Phys. Rev. B* **34**, 3476 (1986).
- [33] K. Davis, M. Mewes, M. Joffe, M. Andrews, and W. Ketterle, *Phys. Rev. Lett.* **74**, 5202 (1995).
- [34] W. Ketterle and N. J. van Druten, *Adv. At. Mol. Opt. Phys.* **37**, 181 (1996).
- [35] D. McKay and B. DeMarco, *Rep. Prog. Phys.* **054401** (2010), 10.1088/0034-4885/74/5/054401.
- [36] W. S. Bakr, J. I. Gillen, A. Peng, S. Fölling, and M. Greiner, *Nature* **462**, 74 (2009).
- [37] F. Serwane, G. Zürn, T. Lompe, T. B. Ottenstein, A. N. Wenz, and S. Jochim, *Science* **332**, 336 (2011).
- [38] B. Zimmermann, T. Müller, J. Meineke, T. Esslinger, and H. Moritz, *New J. Phys.* **13**, 043007 (2011).
- [39] R. Bourgain, J. Pellegrino, A. Fuhrmanek, Y. R. P. Sortais, and A. Browaeys, *Phys. Rev. A* **88**, 023428 (2013).
- [40] H.-P. Breuer and F. Petruccione, *The theory of open quantum systems*. (Oxford University Press, 2002).
- [41] C. Gardiner and P. Zoller, *Quantum noise*., Vol. 56 (Springer, 2004).
- [42] A. M. Shakirov, S. V. Tsibulsky, A. E. Antipov, Y. E. Shchadilova, and A. N. Rubtsov, *Sci. Rep.* **5**, 8005 (2015).
- [43] M. Rigol, *Phys. Rev. A* **80**, 053607 (2009).
- [44] W. Beugeling, R. Moessner, and M. Haque, *Phys. Rev. E* **91**, 012144 (2015).
- [45] T. N. Ikeda, Y. Watanabe, and M. Ueda, *Phys. Rev. E* **87**, 012125 (2013).
- [46] R. Steinigeweg, J. Herbrych, and P. Prelovšek, *Phys. Rev. E* **87**, 012118 (2013).
- [47] W. Beugeling, R. Moessner, and M. Haque, *Phys. Rev. E* **89**, 042112 (2014).

Quantum statistical ensemble for emissive correlated systems (supplementary materials)

Alexey M. Shakirov,^{1,2} Yulia E. Shchadilova,¹ and Alexey N. Rubtsov^{1,2}

¹ Russian Quantum Center, Novaya 100, 143025 Skolkovo, Moscow Region, Russia

² Department of Physics, Lomonosov Moscow State University, Leninskie gory 1, 119991 Moscow, Russia

HILBERT SPACE AND TRANSITIONS

The Hilbert space of the system can be represented as the graph as shown in Fig. S1. Vertices of this graph represent many-body eigenstates $|N, n\rangle$ which are classified by the number of particles N and the energy E_n . Directed edges connect these vertices according to transitions between eigenstates generated by the coupling to the vacuum reservoir. The dynamics of the system can be considered as a walk through the graph. Transitions should satisfy two constraints: (i) $\Delta N = -1$, (ii) $\Delta E < -\varepsilon_0$. By possible transitions we mean all transitions satisfying the first constraint. We divide them into allowed transitions which also satisfy the second constraint and forbidden transitions which do not satisfy the second constraint. We also introduce two categories for the eigenstates of the system. For a given initial state we define an achievable eigenstate as an eigenstate which can be reached from the initial one through allowed transitions. We define a stable eigenstate as an eigenstate from which no further transitions are allowed. Only achievable stable eigenstates are present in the steady state of the system.

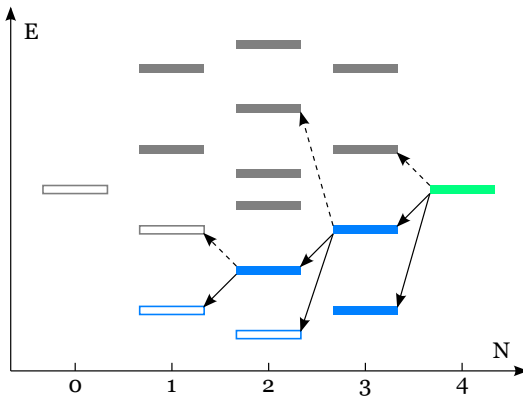


Figure S1. Graphical representation of the Hilbert space. The system of hard-core bosons on a lattice of 4 sites is considered. Bars representing many-body eigenstates $|N, n\rangle$ are placed into the coordinate system ‘number of particles - energy’. Initial maximally occupied pure state is indicated by the green colour. Allowed transitions and some forbidden transitions for $\varepsilon_0 = 0$ are shown with solid and dashed arrows correspondingly. The achievable eigenstates are indicated with the blue colour. The stable eigenstates are represented with empty bars. After the loss of particles the systems in the ensemble can be in either the lowest energy 2-particle eigenstate or the lowest energy 3-particle eigenstate.

BINDING ENERGY

The binding energy ε_0 determines allowed transitions and eigenstates which are present in the steady state of the system. The dependence of the number of these eigenstates on ε_0 for the initial maximally occupied pure state is shown in Fig. S2. For extreme values of the binding energy there is only one achievable stable eigenstate: (i) an empty eigenstate for $\varepsilon_0 = -\infty$ (all possible transitions are allowed), (ii) a maximally occupied eigenstate for $\varepsilon_0 = \infty$ (all possible transitions are forbidden). For calculations we set $\varepsilon_0 = 0$ which corresponds to the maximal value of the number of eigenstates present in the steady state of the system.

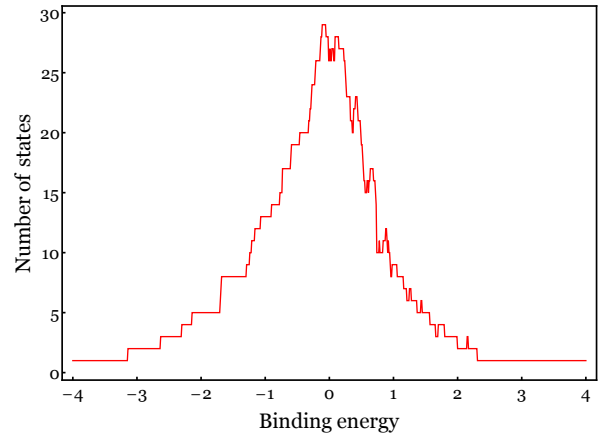


Figure S2. Number of achievable stable eigenstates. The system of hard-core bosons on a 14-site lattice is prepared in the maximally occupied pure state. The plot shows the number of achievable stable eigenstates as the function of the binding energy.

DEPENDENCE ON THE INITIAL ENERGY

As stated in the paper, the steady state of the system is characterized in each sector by the Boltzmann distribution. Here we demonstrate that variation of the initial state of the system only changes parameters of the stationary distribution but not its shape. Fig. S3 shows stationary distributions for initial pure states with $N_0 = 12$ particles and different energies E_0 . We observe that (i) temperatures T_N increase as E_0 increases, (ii) for initial states with close energies stationary distributions are similar.

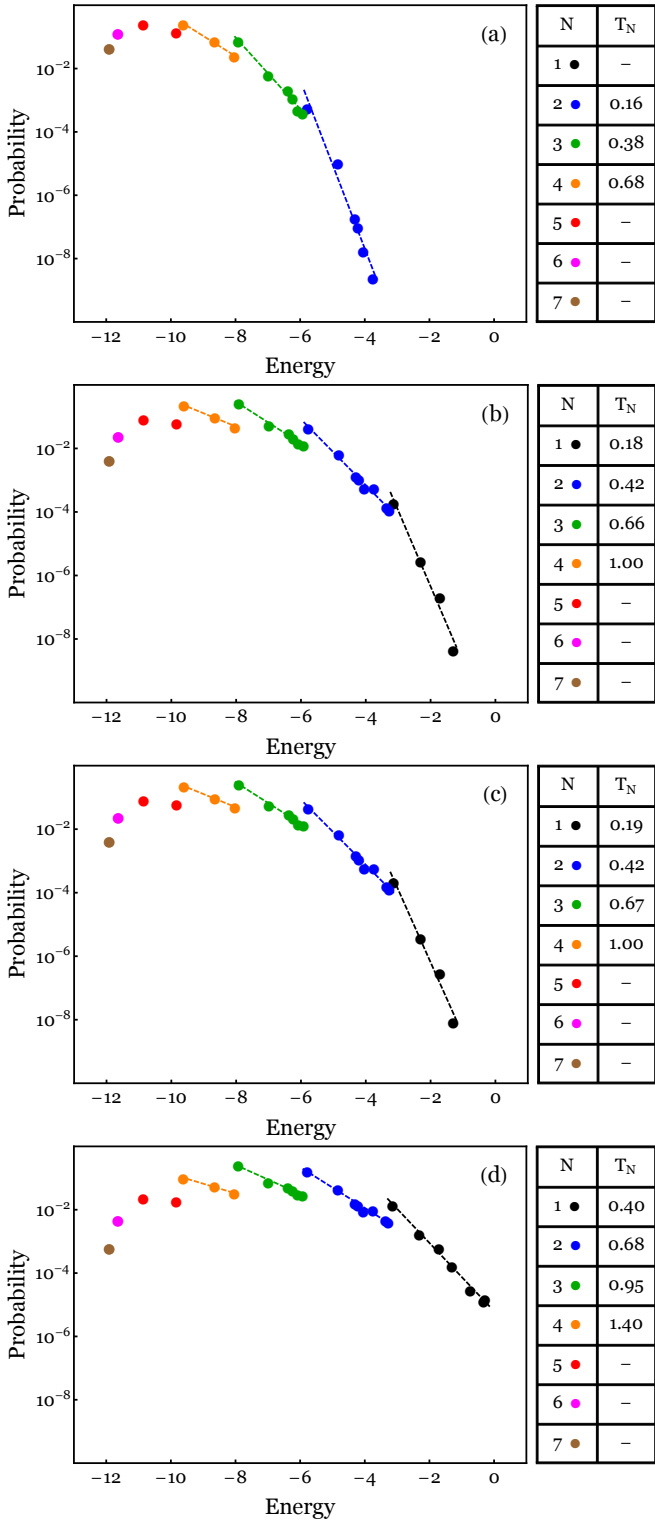


Figure S3. Stationary distributions. The system is prepared in pure states with $N_0 = 12$ particles and different energies: (a) $E_0 = -3.00$, (b) $E_0 = -0.06$, (c) $E_0 = 0.06$, (d) $E_0 = 3.00$. The stationary distributions are of the Boltzmann form in each N -particle sector for all these initial conditions (temperatures are presented in tables).

SCALING ANALYSIS

The amplitude of state-to-state fluctuations of the transition rate as the function of the transition energy depends on the size of the system. Fig. S4 shows that the standard deviation of state-to-state fluctuations becomes smaller as the size of the system increases. Lattices of different sizes are obtained by taking out sites from the 14-site lattice under study.

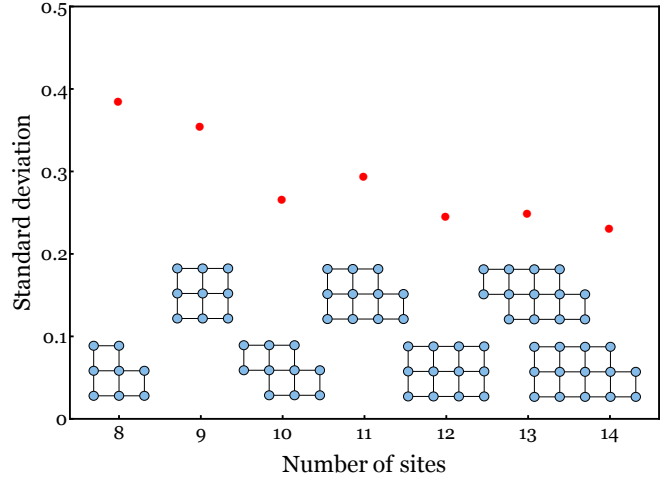


Figure S4. Scaling analysis. The plot shows the standard deviation of $\log_{10}R$ in the interval of transition energies $[-0.1, 0.1]$ as the function of the number of sites in the lattice. Geometries of the lattices of different sizes are shown in the inset.

COOLING/HEATING EFFECT

Preparation of the system in a Gibbs state with $N_0 < 14$ allows us to study the cooling/heating effect in the system and its dependence on the initial temperature T_0 . Fig. S5 shows the inverse temperature $1/T$ as a function of N for Gibbs states with $N_0 = 12$ and different initial temperatures. The energy spectrum of the system is bounded both from below and above, so initial states with negative T_0 can also be considered. In case of negative initial temperatures the system always cools down as particles escape. In case of small positive initial temperatures the loss of the first particle leads to the abrupt heating of the system. This is explained by the shift between spectra of neighbouring sectors which leads to the possibility of transitions from the lowest energy state in N -particle sector to excited ($N-1$)-particle states. For the system under study this condition can be satisfied only for $N > 7$ so that no heating is observed below half-filling. Fig. S5 shows intermediate distributions for systems initially prepared in a Gibbs state and their approximation by the exponential function of energy.

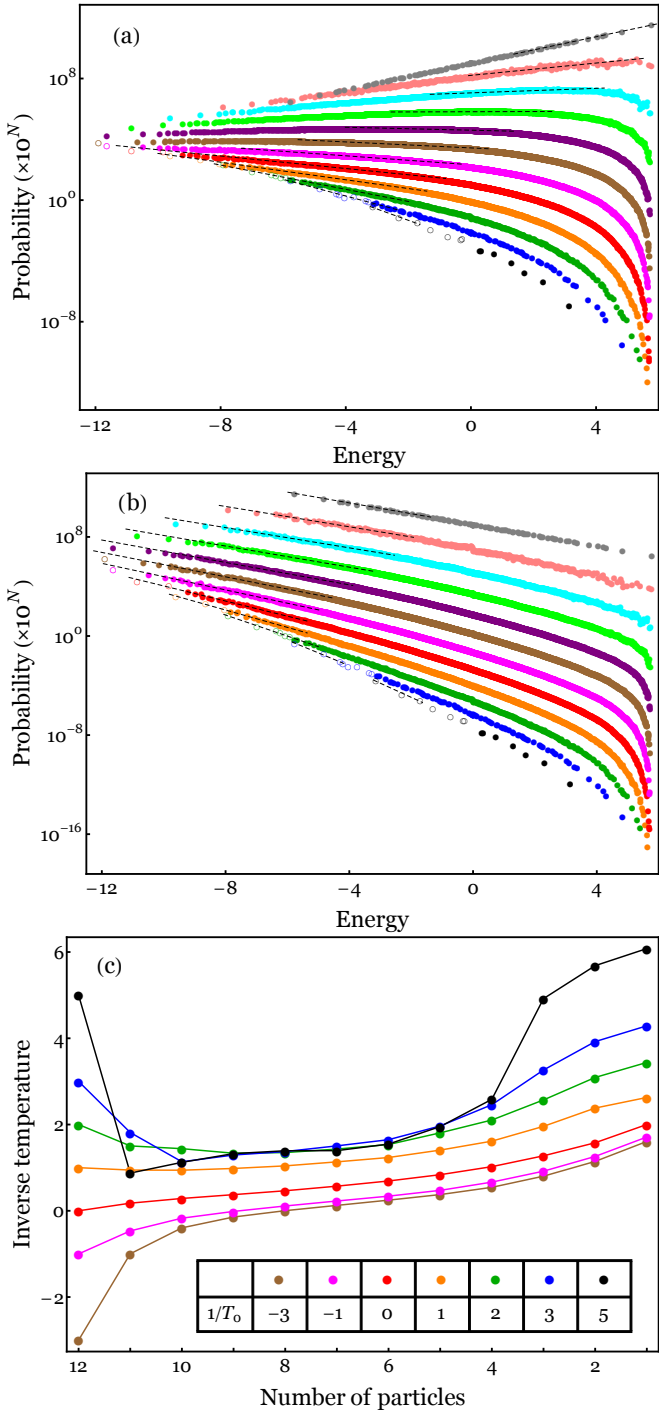


Figure S5. Cooling/heating effect. The plots (a)-(b) show intermediate distributions for the system prepared in the Gibbs state with $N_0 = 12$ and (a) $1/T_0 = -1$, (b) $1/T_0 = 1$. Points accumulating 80% of the total probability in each sector are approximated by exponential functions $P_N(E) \propto \exp(-E/T_N)$. The plot (c) shows the dependence of temperatures T_N on the number of particles for different initial temperatures T_0 . For illustrative purposes N -axis is reversed and temperatures are inverted.